(Received 19 April 2026, Accepted 8 June 2026, Scheduled 26 June 2026)

Hybrid BAS-PSO with Adaptive Weight and Cauchy Mutation of Mean Optimal Position for PMSM Parameter Identification under Inverter Nonlinearity

Yang Zhang, Gao Tang, and Ying Chen*

Hunan University of Technology, Zhuzhou, 412007, China

ABSTRACT: A permanent magnet synchronous motor (PMSM) parameter identification method based on adaptive mean position beetle particle swarm optimization (AMBPSO) is proposed, incorporating the distortion voltage induced by the nonlinearity of the voltage source inverter (VSI) into the parameter set to be identified. An adaptive inertia weighting strategy is designed to improve PMSM parameter identification accuracy and reduce computational time. In addition, the Cauchy mutation average optimal-position strategy is introduced to solve the problem of convergence of the algorithm to a suboptimal solution. Meanwhile, the beetle antenna search (BAS) algorithm is integrated with the improved particle swarm optimization (PSO) strategy, which effectively enhances the particle's dynamic perception of the environment space during the iterative process. The proposed AMBPSO strategy enables each particle to update its speed based on its individual historical optimum, population global optimum, and the beetle tentacle gradient search ability in the iterative process, realizing adaptive exploration of the solution space. Simulated and experimental results demonstrate that, in comparison to traditional PSO, the identification results after distortion voltage compensation are more accurate, and the proposed method significantly enhances identification precision and accelerates convergence speed.

1. INTRODUCTION

Recently, permanent magnet synchronous motors (PMSMs) have been widely used in industrial robots, servo drive systems, high-speed railways, and new energy power generation owing to their high efficiency, high power density, and good dynamic performance [1, 2]. To ensure a proper operation of the PMSM system, accurate electrical parameters are critical for condition monitoring, fault detection, and control system design [3]. Because PMSM is a strongly coupled, nonlinear, time-varying system, its parameters are affected by environmental conditions (such as temperature and load), which makes it difficult to accurately estimate these parameters [4, 5]. For example, when temperature increases, the winding resistance increases, which in turn affects the current conduction and torque generation [6]. Changes in the d-q axis inductance can cause torque ripples that affect the smoothness of motor operation [7]. The demagnetization phenomenon may lead to a decrease in the magnetic flux of the permanent magnet, which will reduce the amplitude of the fundamental back EMF, thereby affecting the speed control and output power of the motor [8]. Therefore, the accurate knowledge of electrical parameters is essential for improving the control performance of the PMSM drive system.

Methods for PMSM parameter identification mainly include offline estimation [9] and online estimation [10]. The offline identification technique only performs the initial parameter identification before motor operation, which cannot realize the immediate identification of PMSM parameters, so it is difficult to effectively solve the problem that the control effect decreases due to parameter changes [11]. Online identification technology is able to estimate the motor's operating parameters in real time according to the operating conditions, thus improving the accuracy and effectiveness of control; therefore, online identification has attracted increasing attention. At present, common online identification methods include Extended Kalman Filter (EKF) [12, 13], recursive least squares (RLS) [14], Model Reference Adaptive System (MRAS) [15, 16], Genetic Algorithm (GA) [17, 18], etc. In [13], by taking the nonlinearity of the voltage source inverter (VSI) as the system state, two online identification schemes of PMSM based on EKF are proposed. However, due to the algorithm's sensitivity to noise, its application is hindered, which requires a large amount of matrix and vector operations, and the process is more intricate. In [14], the RLS method is used to simultaneously estimate the stator resistance, d-q axis inductance, and flux of the motor. Two motor parameters are recognized for each voltage function in the α-β coordinate system. The experimental results show that the method has the advantages of fast convergence and high accuracy. In [15], MRAS is used to estimate the speed and rotor position of the motor, and a neural network is used to identify the motor parameters online. However, MRAS has a strong dependence on motor parameters, which vary with the environment, operating state, etc. In [17], an improved operator-based genetic algorithm for PMSM parameter identification is proposed. Experimental results show that the proposed method achieves global optimization, which can further enhance the algorithm's convergence speed and identification accuracy. However, due

* Corresponding author: Ying Chen (25806448 @qq.com).

to the complexity of the fitness function, the computation time is significantly increased.

The particle swarm algorithm (PSO) has been widely applied to the parameter identification of PMSMs owing to its simple principle, fast computational speed, and parallel optimization in the solution space. A nonlinear decreasing strategy was designed to optimize the PSO inertia weights in [19], and the results showed that PSO discrimination performance was improved, but still could not jump out of the suboptimal solution. Fuzzy particle swarm algorithms in [20] are used to expand the range of influence of individual particles so that the optimization-seeking speed of the particles is affected by multiple surrounding particles, effectively avoiding the population plunging into sub-optimal solutions. To ensure the diversity of the algorithm, the dynamic sample learning strategy, nonlinear multi-scale cross-learning operator, and dynamic opposition learning strategy were improved in [21], which accelerated the convergence efficiency and improved the identification accuracy. However, the algorithm improvement is too complex, and its practical application range is limited. In [22], the VSI dead time affects its identification accuracy, and a shrinkage factor anti-predator particle swarm algorithm is proposed based on time error compensation. The results show that the method improves identification accuracy but is prone to premature maturity.

The beetle antennae search (BAS) algorithm is an intelligent optimization algorithm proposed by Jiang and Li [23]. It differs from other bionic class algorithms in that it is a monolithic search algorithm, which has the strengths of a simple concept and few factors. In [24], a modified BAS algorithm was applied to optimize a fuzzy proportional integral derivative controller, and a new control model of a PMSM drive electric steering gear was established, which enhanced the servo control performance of the PMSM. Because the BAS algorithm has good global search capability, it can complement the strengths and weaknesses when combined with other intelligent algorithms. In [25], the BAS was integrated with the grey wolf algorithm (GWO), which prevents the GWO from falling into local optima during later iterations and effectively improves positioning accuracy and stability in wireless sensor networks. In [26], PSO and BAS were combined to give full play to their advantages, which effectively improved the global optimal escape ability, convergence accuracy, and stability of each dimension. Evidently, the hybrid algorithm strategy is conducive to achieving a better balance between convergence speed and accuracy, thereby improving the overall optimization of the algorithm.

In this study, based on the consideration of VSI nonlinearity, adaptive inertia weights and Cauchy mutation average optimal position were used to improve the identification precision and convergence speed of PSO. A BAS for judging its own environment is added so that the particle introduces its judgment of the environment in the iterative process. That is, the PMSM's parameter identification is based on the adaptive mean position beetle particle swarm algorithm (AMBPSO) considering VSI nonlinear factors. The simulation and experimental results show that the identification accuracy of motor parameters is improved by approximately 1.4% after considering the inverter distortion voltage. After the algorithm improvement, the AMBPSO strategy proposed in this study saved approximately 0.12 s of recognition time and reduced the maximum error by 5.7%.

2. PMSM MATHEMATICAL MODEL

For simplicity and to focus on the influence of VSI nonlinearity on PMSM parameter identification, a simplified PMSM voltage model is adopted in this paper. Several physical factors, including magnetic saturation, spatial harmonics, eddy-current loss, and hysteresis-induced iron loss, are not explicitly considered. For the tested surface-mounted permanent magnet synchronous motor (SPMSM), this simplification is reasonable because the parameter identification experiments are conducted under relatively stable operating conditions and without deep flux-weakening operation. Considering VSI nonlinear factors, the mathematical model of the motor in the d-q coordinate system is expressed as

$$\begin{cases} u_d^* + D_d V_{dead} = R_s i_d + L_d \dfrac{di_d}{dt} - \omega_e L_q i_q \\ u_q^* + D_q V_{dead} = R_s i_q + L_q \dfrac{di_q}{dt} + \omega_e L_d i_d + \omega_e \psi_f \end{cases} \tag{1}$$

where u_d^* and u_q^* are the output voltages of the current controller; i_d and i_q are the d-q axis currents; L_d and L_q are the d-q axis inductances; R_s, L_d, L_q, and ψ_f are the stator resistance, direct and quadrature axis inductances, and permanent magnet flux, respectively; ω_e is the rotor electrical angular velocity; D_d and D_q are periodic functions of rotor position, which are expressed as

$$\begin{bmatrix} D_d \\ D_q \end{bmatrix} = 2 \begin{bmatrix} \cos(\theta) & \cos(\theta - \frac{2\pi}{3}) & \cos(\theta + \frac{2\pi}{3}) \\ -\sin(\theta) & -\sin(\theta - \frac{2\pi}{3}) & \sin(\theta - \frac{\pi}{3}) \end{bmatrix} \times \begin{bmatrix} \text{sign}(i_{as}) \\ \text{sign}(i_{bs}) \\ \text{sign}(i_{cs}) \end{bmatrix} \tag{2}$$

In Eq. (2), i_{as}, i_{bs}, and i_{cs} are the three-phase current of stator ABC, and

$$\text{sign} = \begin{cases} 1, & i \geq 0 \\ -1, & i < 0 \end{cases} \tag{3}$$

V_{dead} is the distortion voltage caused by VSI nonlinearity, which can be expressed as

$$V_{dead} = \frac{\mathrm{T_{dead}} + \mathrm{T_{on}} - \mathrm{T_{off}}}{\mathrm{T_s}} (\mathrm{V_{dc}} - \mathrm{V_{sat}} + \mathrm{V_{dd}}) + \frac{\mathrm{V_{sat}} + \mathrm{V_{dd}}}{2} \tag{4}$$

For the SPMSM, there is $L_d = L_q = L_s$. When the SPMSM operates stably, the disturbances in i_d and i_q are minimal, and the steady-state voltage equation can be expressed as

$$\begin{cases} u_d^* + D_d V_{dead} = R_s i_d - \omega_e L_s i_q \\ u_q^* + D_q V_{dead} = R_s i_q + \omega_e L_s i_d + \omega_e \psi_f \end{cases} \tag{5}$$

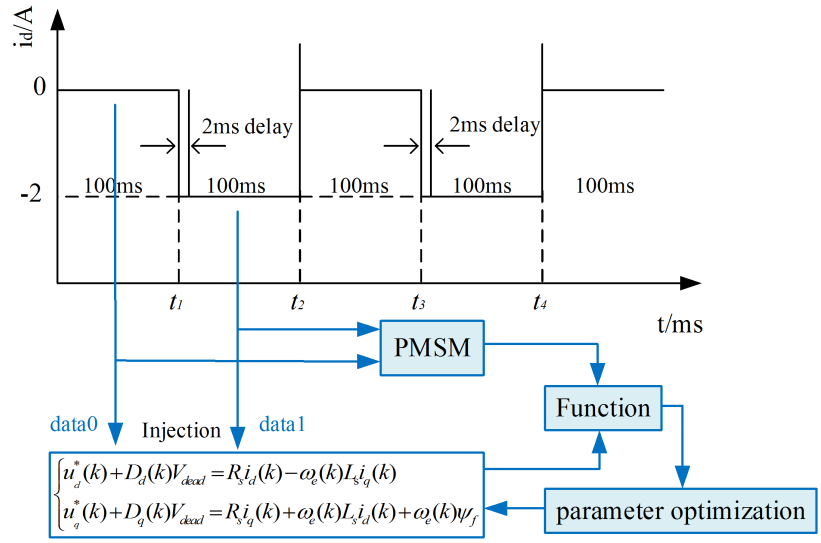

FIGURE 1. Data sampling diagram.

Because the electrical parameters (R_s, L_s, ψ_f) and distortion voltage (V_{dead}) need to be identified, but the order of the motor voltage equation in the steady state is less than the parameters that need to be identified, it cannot meet the requirements of simultaneous online recognition. Therefore, the issue of rank deficiency in the equations must be resolved.

3. DESIGN OF PMSM PARAMETER IDENTIFICATION MODEL

To address the issue of rank deficiency in the system of equations, a method of feeding a negative current ($i_d = -2$) on the d-axis is adopted. First, the data at $i_d = 0$ are collected, that is, data 0, and then the corresponding data1 are collected 2 ms after the negative sequence current ($i_d = -2$) is injected. The 2 ms delay before starting to measure data1 ensures that measurements were made after the step transient associated with the i_d pulse was established, ensuring reliable data acquisition. The data acquisition diagrams for the two modes are shown in Fig. 1.

Therefore, by collecting the same amount of data in both states, two sets of d-q equations are obtained, as shown in (6)

$$\begin{cases} u_{d0}^*(k) + D_{d0}(k)V_{dead} = -\omega_{e0}(k)L_s i_{q0}(k) \\ u_{q0}^*(k) + D_{q0}(k)V_{dead} = R_s i_{q0}(k) + \omega_{e0}(k)\psi_f \\ u_{d1}^*(k) + D_{d1}(k)V_{dead} = R_s i_{d1}(k) - \omega_{e1}(k)L_s i_{q1}(k) \\ u_{q1}^*(k) + D_{q1}(k)V_{dead} = R_s i_{q1}(k) + \omega_{e1}(k)L_s i_{d1}(k) + \omega_{e1}(k)\psi_f \end{cases} \tag{6}$$

where the variable subscripted "0" indicates that it is under the control strategy with $i_d = 0$, and the variable subscripted "1" indicates that it is under the control strategy with $i_d = -2$.

The adjustable model is designed as

$$\begin{cases} \hat{u}_{d0}^*(k) + D_{d0}(k)\hat{V}_{dead} = -\omega_{e0}(k)\hat{L}_s i_{q0}(k) \\ \hat{u}_{q0}^*(k) + D_{q0}(k)\hat{V}_{dead} = \hat{R}_s i_{q0}(k) + \omega_{e0}(k)\hat{\psi}_f \\ \hat{u}_{d1}^*(k) + D_{d1}(k)\hat{V}_{dead} = \hat{R}_s i_{d1}(k) - \omega_{e1}(k)\hat{L}_s i_{q1}(k) \\ \hat{u}_{q1}^*(k) + D_{q1}(k)\hat{V}_{dead} = \hat{R}_s i_{q1}(k) + \omega_{e1}(k)\hat{L}_s i_{d1}(k) + \omega_{e1}(k)\hat{\psi}_f \end{cases} \tag{7}$$

where $\hat{u}_{d0}^*(k)$, $\hat{u}_{q0}^*(k)$, $\hat{u}_{d1}^*(k)$ and $\hat{u}_{q1}^*(k)$ are the stator voltages of the adjustable model in d-axis and q-axis.

Based on this, this study introduces a novel fitness function that can realize the response fitting of the two models (actual and adjustable) under a given input. It can be written as

$$\begin{cases} f_1(k)[\hat{L}_s, \hat{V}_{dead}] = K^{-1}[u_{d0}^*(k) - \hat{u}_{d0}^*(k)]^2 \\ f_2(k)[\hat{R}_s, \hat{\psi}_f, \hat{V}_{dead}] = K^{-1}[u_{q0}^*(k) - \hat{u}_{q0}^*(k)]^2 \\ f_3(k)[\hat{R}_s, \hat{L}_s, \hat{V}_{dead}] = K^{-1}[u_{d1}^*(k) - \hat{u}_{d1}^*(k)]^2 \\ f_4(k)[\hat{R}_s, \hat{\psi}_f, \hat{L}_s, \hat{V}_{dead}] = K^{-1}[u_{q1}^*(k) - \hat{u}_{q1}^*(k)]^2 \end{cases} \tag{8}$$

where K represents the maximum number of iterations in the algorithm.

The optimal parameters can be simultaneously identified in this process, and the fitness function can be simplified to

$$f(k)[\hat{R}_s, \hat{L}_s, \hat{\psi}_f, \hat{V}_{dead}] = \sum_{i=1}^{4} a_i f_i(k) \tag{9}$$

where a_i represents the weight coefficient of each fitness subfunction, respectively. Considering the strong coupling relationship among equations and identification parameters and the importance of each parameter's accuracy, weighting coefficients with equal weights were chosen, that is, $a_i = 0.25$.

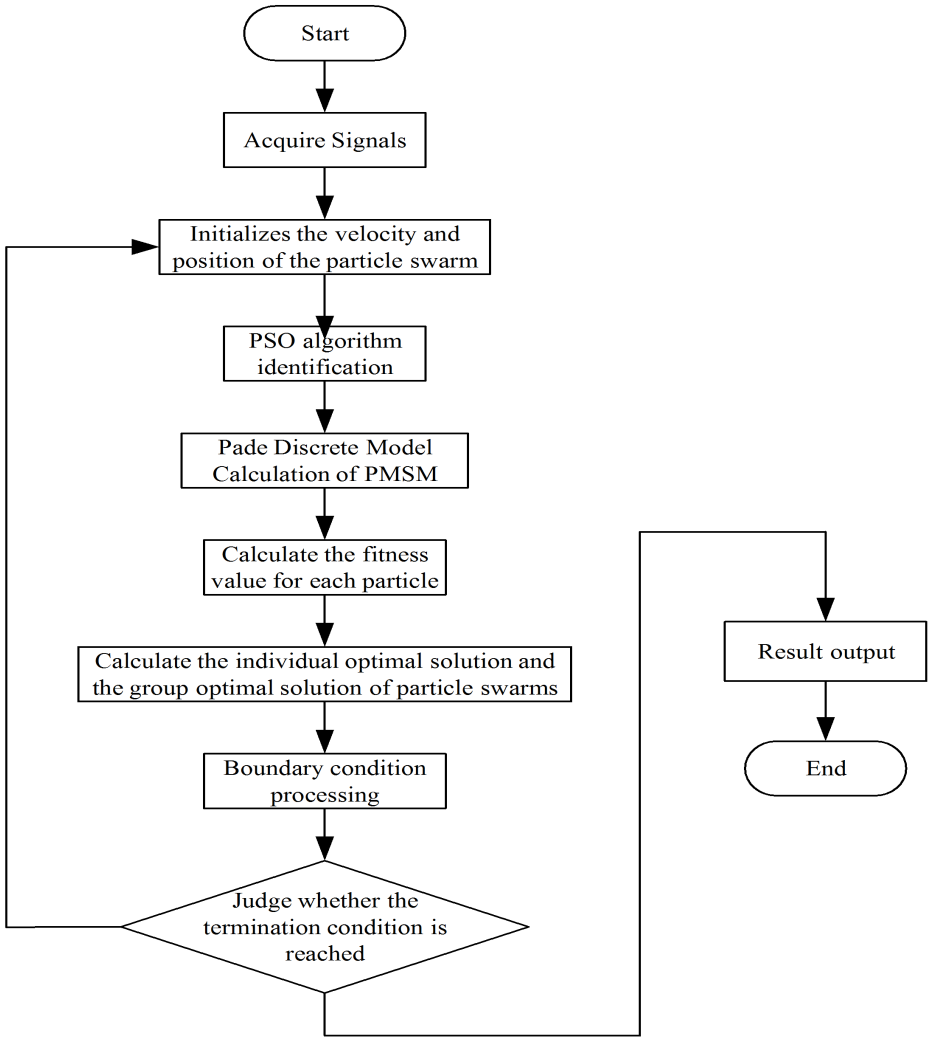

FIGURE 2. PSO parameter identification flow diagram.

4. PSO OPTIMIZATION

4.1. Basic PSO

PSO is an optimization algorithm that simulates the foraging activities of birds. It is commonly applied in the field of PMSM parameter identification because of its uncomplicated algorithm, strong search ability, and rapid convergence speed. The fundamental idea of the algorithm is to find the optimal solution by simulating birds' foraging behavior through particle movement and mutual information sharing. Suppose that there are n particles in a D-dimensional search space, and each particle generates a velocity vector and a position vector to gradually approach the optimal position. The search equation is

$$\begin{cases} v_i^{k+1} = \omega v_i^k + c_1 r_1 (P_{best}^k - x_i^k) + c_2 r_2 (G_{best}^k - x_i^k) \\ x_i^{k+1} = x_i^k + v_i^{k+1} \end{cases} \tag{10}$$

where v_i and x_i correspond to the position and velocity of particle i; P_{best} is the individual perfect solution; G_{best} is the group perfect solution; k corresponds to the number of iterations; r_1, r_2 are random variables within the interval [0, 1]; c_1, c_2 correspond to the individual and group learning coefficients, respectively, with ω being the inertia weight.

The flowchart of the basic PSO used for identification is shown in Fig. 2.

4.2. Adaptive Inertia Weight PSO

The inertia weight determines the extent to which a particle's previous velocity influences its current iteration. A larger inertia weight helps enhance the global search ability, enabling particles to escape from local optima. A smaller inertia weight tends to local contraction to increase its convergence speed. In the basic PSO, the inertia weights are set to a fixed constant. In adaptive inertia weighting PSO (APSO), the inertia weight optimization changes with the size of the current particle adaptation. When the current particle adaptation is less than the average adaptation of all particles, the corresponding inertia weight factor is small, thus retaining the particle to continue the local exploration. Conversely, when the self-adaptation of the current particle is greater than the average self-adaptation of all particles, the corresponding inertia weight factor is larger, so

that the particle explores globally in other directions. The strategy is defined as APSO, which is represented by the following formula:

$$\omega = \begin{cases} \omega_{\min} + (\omega_{\max} - \omega_{\min}) \dfrac{f - f_{\min}}{f_{avg} - f_{\min}}, & f \le f_{avg} \\ \omega_{\max}, & f > f_{avg} \end{cases} \tag{11}$$

where $\omega_{\max}$ represents the starting inertia weight of 0.9; $\omega_{\min}$ represents the concluding inertia weight of 0.4; f denotes the current adaptive size of the particle; $f_{\min}$ denotes the minimum adaptation of the particle for the current iteration; and f_{avg} denotes the average value of the global particle adaptation.

In APSO, the inertia weight of each particle changes according to the global average fitness and its own fitness value, which not only enables high-quality particles to conduct local refinement but also enhances the search capability of poorer particles, thereby expanding the search range and preventing convergence to local optima.

4.3. Cauchy Mutation Mean Optimal Position PSO

Based on the APSO, the mean optimal position strategy was introduced. The particle flight experiences are learned from the flight experiences of all particles globally. This strategy is the optimal mean position of all particles and is mathematically expressed as:

$$P_{nd} = \frac{1}{n}\sum_{i=1}^{n} P_{id} = \frac{(P_1 + P_2 + P_3 + \ldots + P_n)}{\mathrm{n}} \tag{12}$$

The mean optimal position can search for more global information. When the mean optimal position in the population approaches the steady state and is greater than a certain number of times, the Cauchy mutation has a strong disturbance ability, and the mutation formula is

$$p_{md} = p_{nd}(1 + C\mathrm{auchy}(x_{\mathrm{i}})) \tag{13}$$

$$C\mathrm{auchy}(\mathrm{x_i}) = \frac{1}{\pi(\mathrm{x_i^2} + 1)} \tag{14}$$

P_{md} is the mean optimal position after mutation, and x_i is the position of the particle.

Under AMPSO, the equation is updated as follows:

$$\begin{cases} v_i^{k+1} = \omega v_i^k + c_1 r_1 (P_{\mathrm{md}}^k - x_i^k) + c_2 r_2 (G_{best}^k - x_i^k) \\ x_i^{k+1} = x_i^k + v_i^{k+1} \end{cases} \tag{15}$$

The mutation mean best position P_{md} draws on the experience of other particles while also including its own optimal position, so particles can use more information to decide their actions. In AMPSO, the global search ability is enhanced, and the cooperation among particles and the reference to the experience information of other particles are improved.

4.4. Hybrid BAS-PSO

The PSO may gather near a local optimal solution during the search process, such that the optimal solution cannot be further found. The integration of BAS with robust global search capabilities into PSO can significantly enhance the PSO's optimization capability and help it escape local optima. BAS is a bionic optimization algorithm that mimics the act of beetles using tentacles to explore the environment when they search for food. The algorithm simulates the perceived strength of the two tentacles on the left and right of the beetle at various positions to determine the direction of the next move, to gradually approach the target. During foraging, beetles are drawn to the scent of food, and the two tentacles perceive the food odor in the air. Owing to the disparity in the distance between the food and the two antennae, the concentration of the odor detected by the antennae also varies. When food is located on the right side of the beetle, the odor concentration detected by the right antenna is higher than that detected by the left. Therefore, beetles can navigate towards the side with a higher concentration based on the disparity in the concentration detected by the two antennae.

In the D-dimensional space, the centroid position of the beetle's whiskers is $X(X_1, X_2, \ldots, X_D)$, and the positions of the left and right antennae of the beetle are defined as

$$\begin{cases} X_{\mathrm{r}} = X_{\mathrm{k}} + d_k \bar{b} \\ X_l = X_{\mathrm{k}} - d_k \bar{b} \end{cases} \tag{16}$$

where X_k represents the centroid position of beetles in k iterations; X_r and X_l represent the right and left whiskers, respectively; d_k represents the sensing range of beetles in k iterations; $\bar{b}$ denotes a stochastic unit vector, which requires normalization.

$$\bar{b} = \frac{\mathrm{rands}(D, 1)}{\|\mathrm{rands}(D, 1)\|_2} \tag{17}$$

By comparing the disparity in odor concentration detected by the left and right antennae, the next search ability of the particle (beetle) is described as

$$\hat{X}^k = \delta_k \bar{b} \cdot \mathrm{sign}\left[f(X_r) - f(X_l)\right] \tag{18}$$

where f denotes the fitness function, δ_k the exploration step at the k-th iteration, and *sign* the sign function.

The performance of the BAS depends on the settings of the sensing range d and search step δ. The values of the sensing range d and search step size δ are dynamically updated by incorporating an exponential decay model to satisfy the global search objectives of the algorithm.

$$\begin{cases} d_k = d_0 \theta_d^{\frac{t}{T_d}} \\ \delta_k = \delta_0 \theta_\delta^{\frac{t}{T_\delta}} \end{cases} \tag{19}$$

where d_0 denotes the initial beetle detection range; δ_0 denotes the initial search step size; θ_d and θ_δ are the decay parameters; T_d and T_δ are the exponential decay time constants.

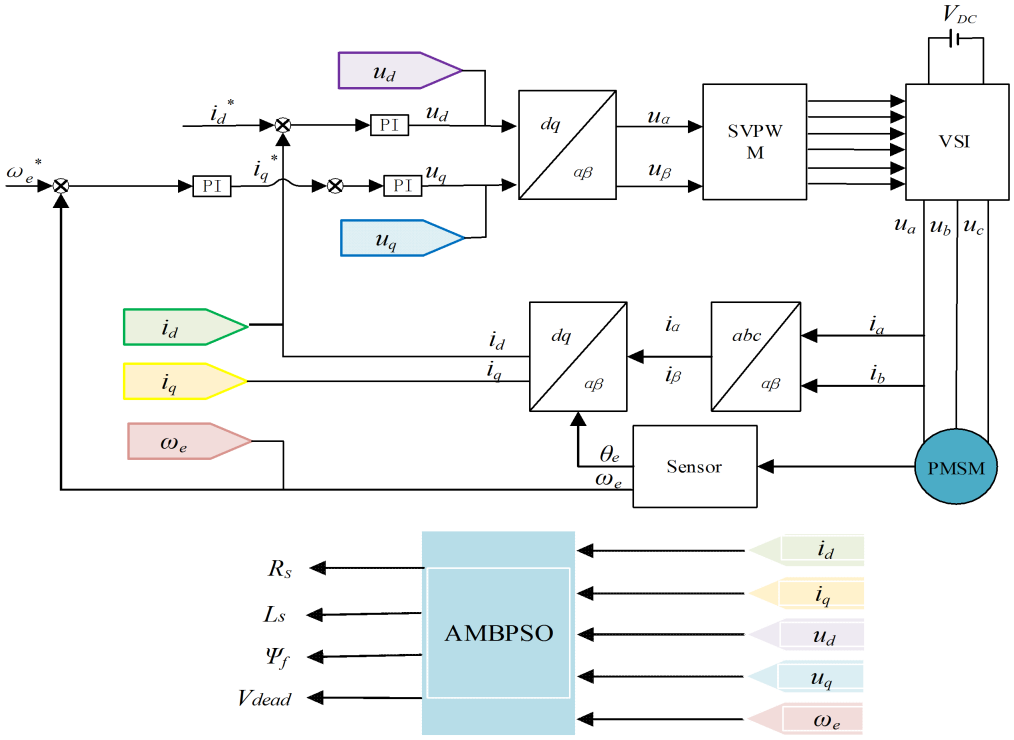

FIGURE 3. Control block diagram under AMBPSO strategy.

In the BAS algorithm, the initial detection range d_0, search step δ_0, and their decay coefficients θ_d and θ_δ have significant effects on the balance between global exploration and local exploitation. Larger initial parameters are beneficial for expanding the search range and avoiding premature convergence but may prolong the convergence time and cause oscillations near the optimal solution. Smaller initial parameters can accelerate local convergence, but may lead to insufficient search ability and increase the risk of falling into local optima. The decay coefficients determine the variation rates of T_d and T_δ, thereby directly affecting the transition from global search to local fine optimization. Therefore, an exponential decay model is adopted in this study to dynamically adjust the detection range and search step, so as to balance the global exploration ability in the early stage and the local identification accuracy in the later stage.

By introducing BAS into AMPSO, each particle increases its ability to judge the environment of BAS based on its own search. Ultimately, its search capabilities are described as

$$\begin{cases} v_i^{k+1} = \omega v_i^k + c_1 r_1 (P_{\text{md}}^k - x_i^k) + c_2 r_2 (G_{best}^k - x_i^k) + c_3 r_3 \hat{X}^k \\ x_i^{k+1} = x_i^k + v_i^{k+1} \end{cases} \tag{20}$$

where c_3 is the BAS learning coefficient, and $r_3 \in [0, 1]$ is a random variable.

5. SIMULATION ANALYSIS

To fully validate the performance of the AMBPSO algorithm in SPMSM parameter identification, a vector control system model based on SPMSM was constructed in the MATLAB/Simulink simulation environment. This model employs a synchronous rotating coordinate system (i.e., the d-q coordinate system) to decompose the motor stator current into excitation and torque components, thereby achieving the decoupled control of flux and torque to improve the system's dynamic response and control accuracy. The overall control structure of the developed system is illustrated in Fig. 3.

The parameters of SPMSM are presented in Table 1.

The population size in the algorithm was 30, and the number of iterations was the ratio of the execution time to the sampling time. The learning factors are set as $c_1 = c_2 = c_3 = 2$, simulation system running time 0.4 s, sampling time 1e-6s. Under different operating conditions (PSO, EKF, RLS, PSO_V, APSO_V, AMPSO_V, AMBPSO_V), the parameters of the SPMSM are identified independently 10 times, and the mean value is regarded as the final output. Meanwhile, to further demonstrate the advantages of the proposed AMBPSO_V algorithm in terms of identification accuracy and convergence performance, the traditional EKF and RLS algorithms are introduced for comparison. Although EKF and RLS are traditional estimation methods commonly used in motor parameter identification, their identification performance is easily affected by model accuracy, initial parameters, noise settings, and the stability of the recursive process. In contrast, PSO-based intelligent optimization algorithms have stronger global search capability and do not rely on strict linearization assumptions. Therefore, through comparative analysis of multiple algorithms, the superiority of the AMBPSO_V algorithm, considering VSI distortion voltage and improved optimization strategies, can be more comprehensively verified in terms of parameter identi-

TABLE 1. PMSM system parameters.

Parameter	Value	Parameter	Value
Pole Pairs	4	Rated Torque (N · m)	15
R_s (Ω)	1.29	T_{on}/ns	80
L_s (mH)	2.53	T_{off}/ns	390
ψ_f (Wb)	0.3	T_{dead}/us	2
Moment of Inertia (kg · m^2)	0.00277	V_{sat}/V	1.8–2.7
Rated Power (kW)	2.3	V_{dd}/V	2.2–3.3
Rated Speed (rpm)	1000	V_{dc}/V	100

TABLE 2. Parameter identification value and error rate.

Parameter	PSO	EKF	RLS	PSO_V	APSO_V	AMPSO_V	AMBPSO_V
R_s (Ω)	1.3667	1.3723	1.3787	1.2322	1.2434	1.3205	1.2663
Error (%)	5.9457	6.3798	6.8760	−4.4806	−3.6124	2.3643	−1.8372
L_s (mH)	2.7211	2.7478	2.7473	2.3618	2.6520	2.5863	2.5857
Error (%)	7.5534	8.4111	8.9842	−6.6482	4.8221	2.2253	2.2016
ψ_f (Wb)	0.3164	0.3182	0.3191	0.3144	0.3117	0.3075	0.2942
Error (%)	5.4667	6.0667	6.3667	4.8000	3.9000	2.5000	−1.9333
V_{dead} (V)	-			−0.3836	−0.3874	−0.4097	−0.3918
Error (%)	-			−4.1000	−3.1500	2.4250	−2.0500

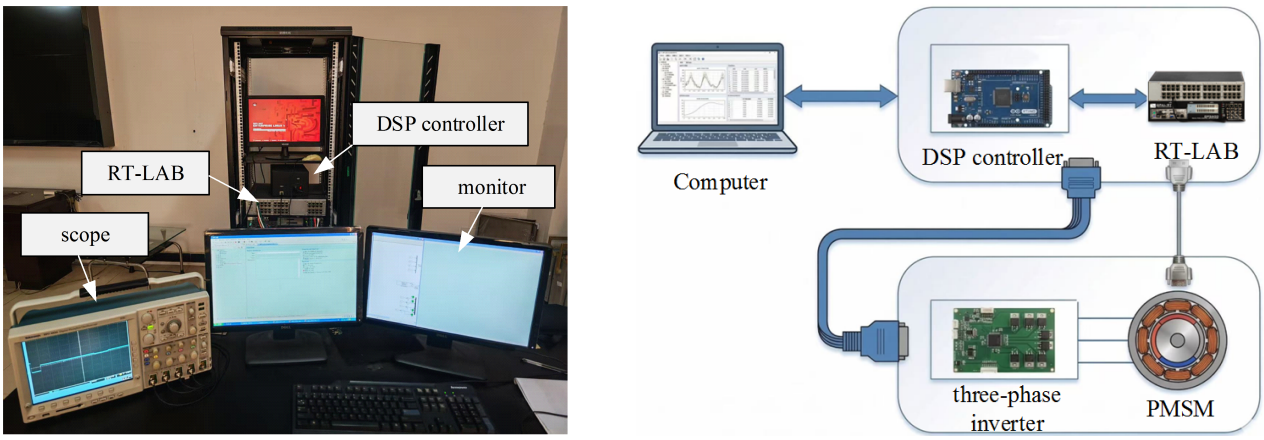

FIGURE 4. Diagram of RT-LAB experimental equipment.

fication accuracy, robustness, and convergence performance. The final simulation results and error rates are listed in Table 2. In the table, the representation of V with a subscript considers the identification results of V_{dead}, and the representation of V without a subscript does not consider the identification results of V_{dead}.

As shown in the table, when VSI distortion voltage is not considered, the identification errors of PSO, EKF, and RLS are relatively large. In particular, the maximum error of the RLS algorithm reaches 8.9842%, indicating that traditional estimation methods have limited identification accuracy under complex nonlinear conditions. After considering the VSI distortion voltage, the identification accuracy of the improved PSO algorithms is significantly enhanced, demonstrating that this strategy can effectively reduce the model error caused by inverter nonlinearity. Among them, the identification errors of the AMBPSO_V algorithm for all motor parameters are basically controlled at around 2%, with a maximum error of only 2.2016%. Compared with PSO, EKF, RLS, and other improved PSO algorithms, AMBPSO_V achieves higher identification accuracy and better stability. This indicates that the introduced adaptive strategy, average-position guidance, and BAS mechanism can effectively improve the search capability of the particle swarm optimization algorithm, enhance its ability to escape

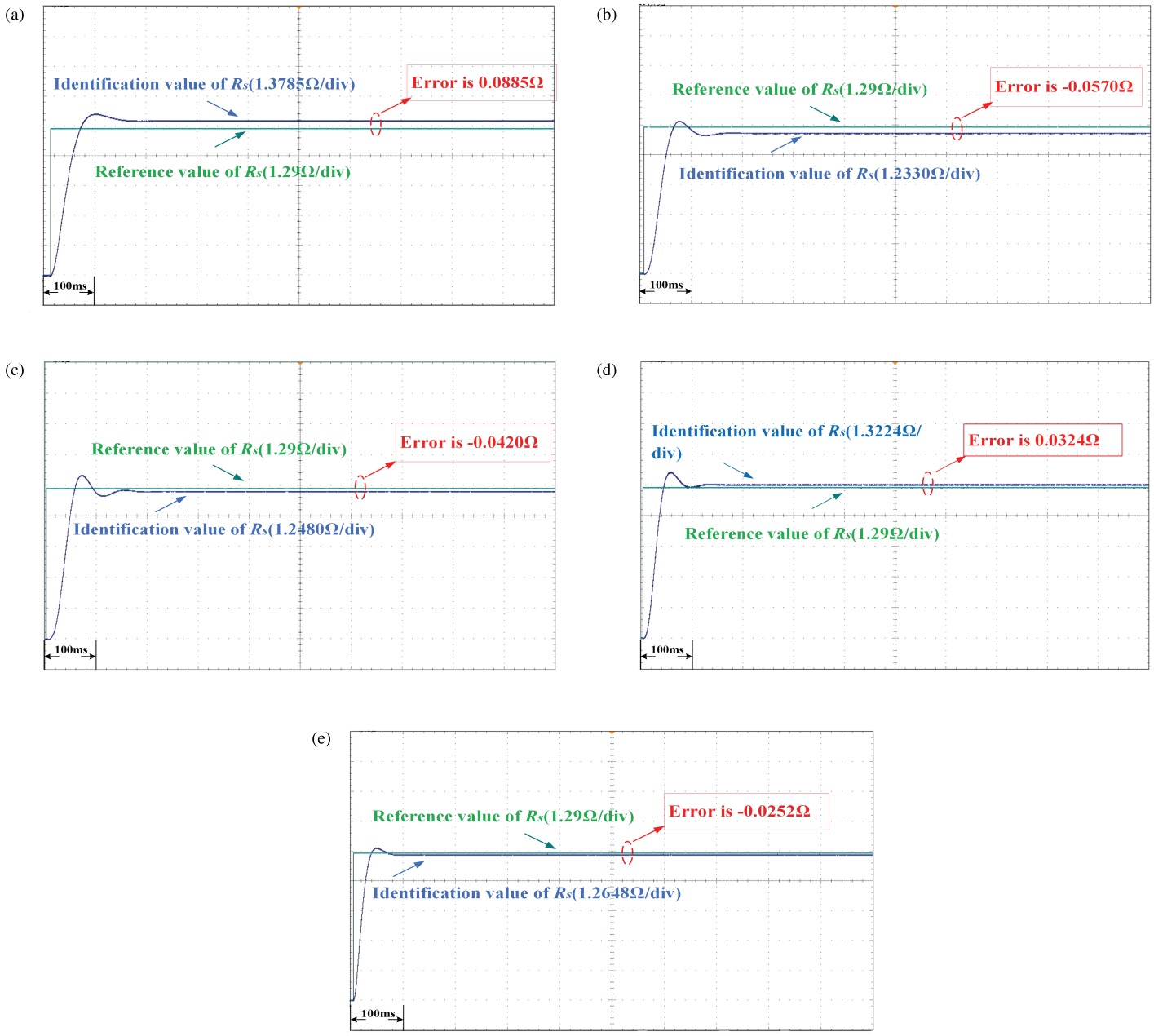

FIGURE 5. The recognition curve of R_s. (a) PSO (100 ms/div), (b) PSO_$_V$ (100 ms/div), (c) APSO_$_V$ (100 ms/div), (d) AMPSO_$_V$ (100 ms/div), and (e) AMBPSO_v (100 ms/div).

from local optima, and thereby improve the accuracy and robustness of SPMSM parameter identification.

6. EXPERIMENTAL ANALYSIS

In Fig. 4, the proposed algorithm is tested on an RT-LAB hardware platform to validate its effectiveness. This platform includes a TMS320F2812DSP controller, an RT-LAB (OP5600) simulator, a motor drive model built in a RT-LAB, a host computer, and an oscilloscope. The RT-LAB was utilized to implement the operation of the VSI and PMSM, and the controller of the running algorithm was TMS320F2812.

(1) Conventional experiment

Using the established experimental platform and under experimental conditions identical to those of the aforementioned simulations, the dynamic convergence curves for the parameters to be identified were measured and are shown in Figs. 5–8. Table 3 lists the specific experimental results obtained using the method described in this study.

From the R_s identification value in Fig. 5, it can be noted that the error rate of the identified results under the basic PSO is relatively large compared to the true value, and the convergence speed is slow. The identification results of the improved algorithm are -4.4186%, -3.2558%, 2.5116%, -1.9535% for the distortion voltages considering the VSI, while the highest identification accuracy is achieved at AMBPSO_$_V$, which is

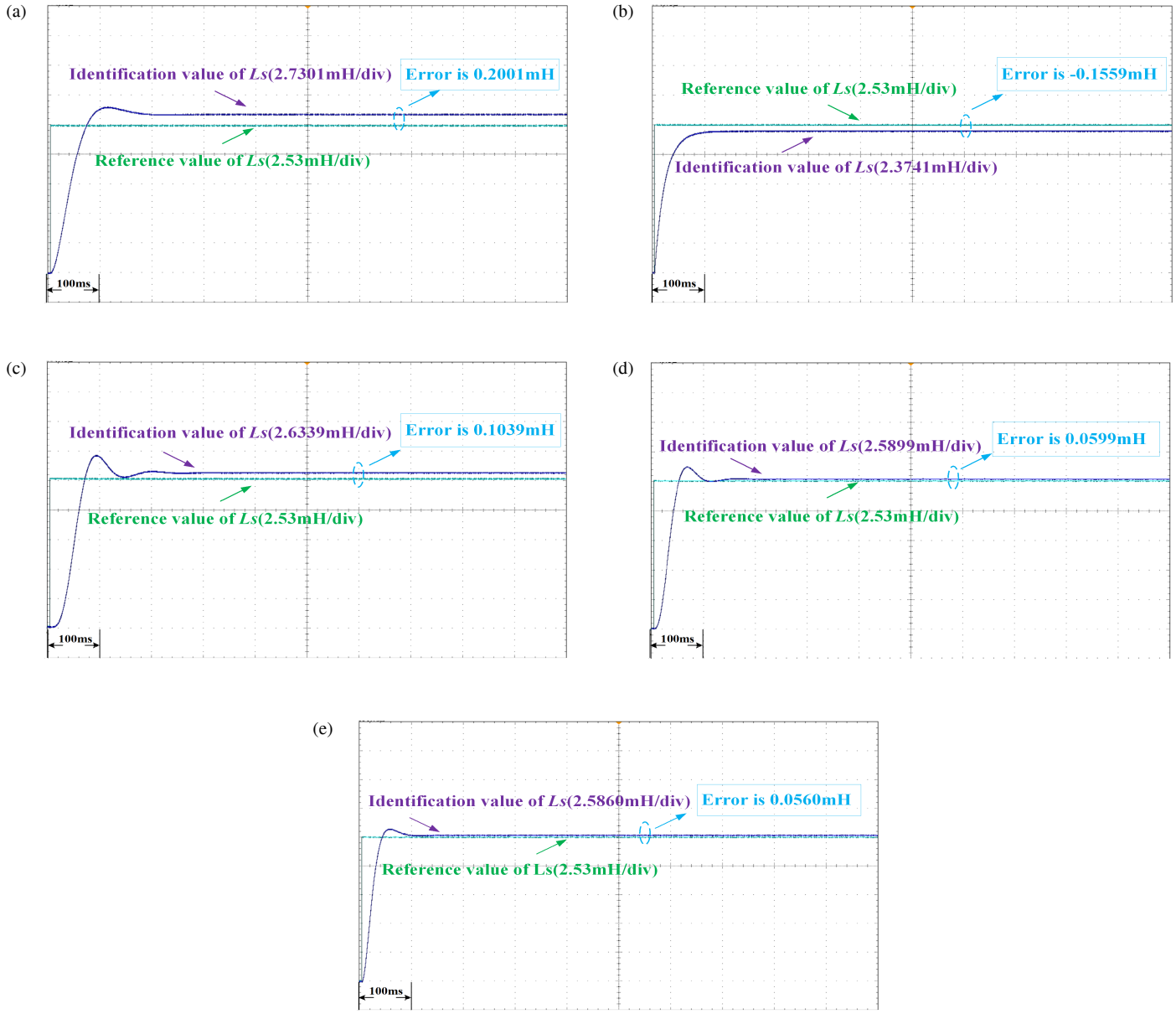

FIGURE 6. The recognition curve of L_s. (a) PSO (100 ms/div), (b) PSO_$_V$ (100 ms/div), (c) APSO_$_V$ (100ms/div), (d) AMPSO_ $_V$ (100 ms/div), and (e) AMBPSO_$_V$ (100 ms/div).

TABLE 3. Motor parameter identification values and error rates under conventional experiments.

Parameter	PSO	PSO_$_V$	APSO_$_V$	AMPSO_$_V$	AMBPSO_$_V$
R_s (Ω)	1.3785	1.2330	1.2480	1.3224	1.2648
Error (%)	6.8605	−4.4186	−3.2558	2.5116	−1.9535
L_s (mH)	2.7301	2.3741	2.6339	2.5899	2.5860
Error (%)	7.9091	−6.1621	4.1067	2.3676	2.2134
ψ_f(Wb)	0.3134	0.3117	0.3102	0.3086	0.2948
Error (%)	4.4667	3.9000	3.0000	2.8667	−1.7333
V_{dead}(V)	-	−0.3826	−0.3863	−0.4095	−0.3915
Error (%)	-	−4.3500	−3.4250	2.3750	−2.1250

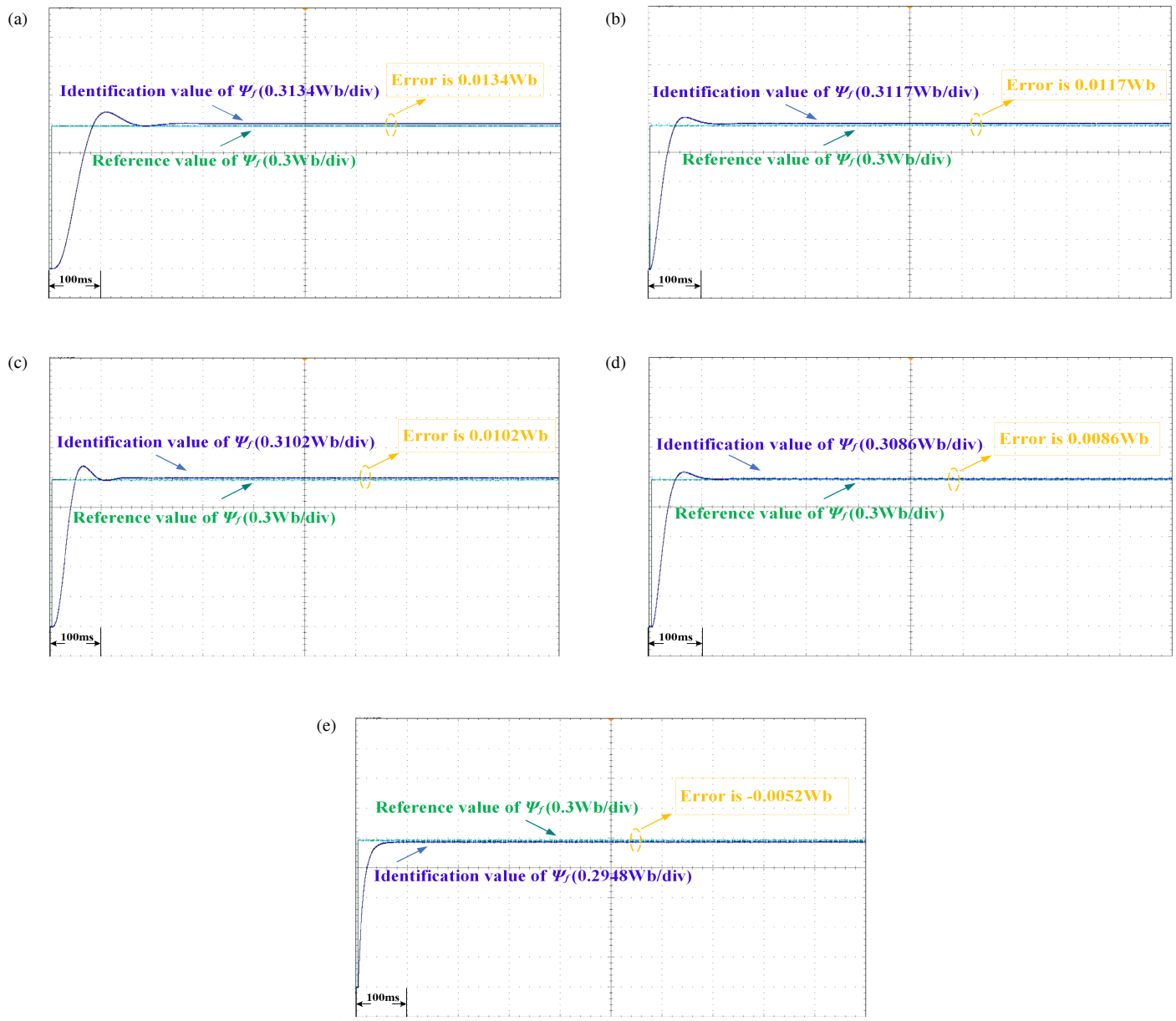

FIGURE 7. The recognition curve of ψ_f. (a) PSO (100 ms/div) (b) PSO_$_V$ (100 ms/div). (c) APSO_$_V$ (100 ms/div). (d) AMPSO_ $_V$ (100 ms/div). (e) AMBPSO_$_V$ (100 ms/div).

reduced by 4.9% compared to the basic PSO. The results of the error percentage for resistor identification under the above five sets of experiments show that AMBPSO_$_V$ can better track the motor's parameter changes in a timely manner.

From the L_s identification value in Fig. 6, it can be observed that the identification result of the inductance under the basic PSO algorithm is 2.7301 mH, with a relative error of 7.9091% compared to the reference value. After the distortion voltage is considered, the discrimination error is reduced by approximately 1.75%, indicating that discrimination accuracy was improved by considering the distortion voltage. Based on this, the algorithm was improved. The error value under APSO_$_V$ was 0.1039 mH, the error value under AMPSO_$_V$ was 0.0599 mH, and the error value under AMBPSO_$_V$ was 0.0560mH. It can be calculated from the accuracy that the error of the improved AMBPSO_$_V$ was reduced by approximately 5.7% compared with that of the basic PSO.

The recognition curve of the flux linkage is depicted in Fig. 7. The convergence time required for the conventional PSO was 227 ms, as analyzed from the timeliness pair identification curve. In contrast, the AMBPSO_$_V$ algorithm proposed in this study significantly compressed the convergence elapsed time to 98 ms and shortened the time cost by 129 ms through a parameter optimization strategy. The PSO_$_V$, APSO_$_V$, and AMPSO_$_V$ took 159 ms, 131 ms, and 119 ms, respectively. AMBPSO_$_V$ has a more optimal recognition time consumption owing to the optimization strategy and hybrid BAS algorithm. Experimental data show that the algorithm has significant advantages in terms of both convergence stability and computa-

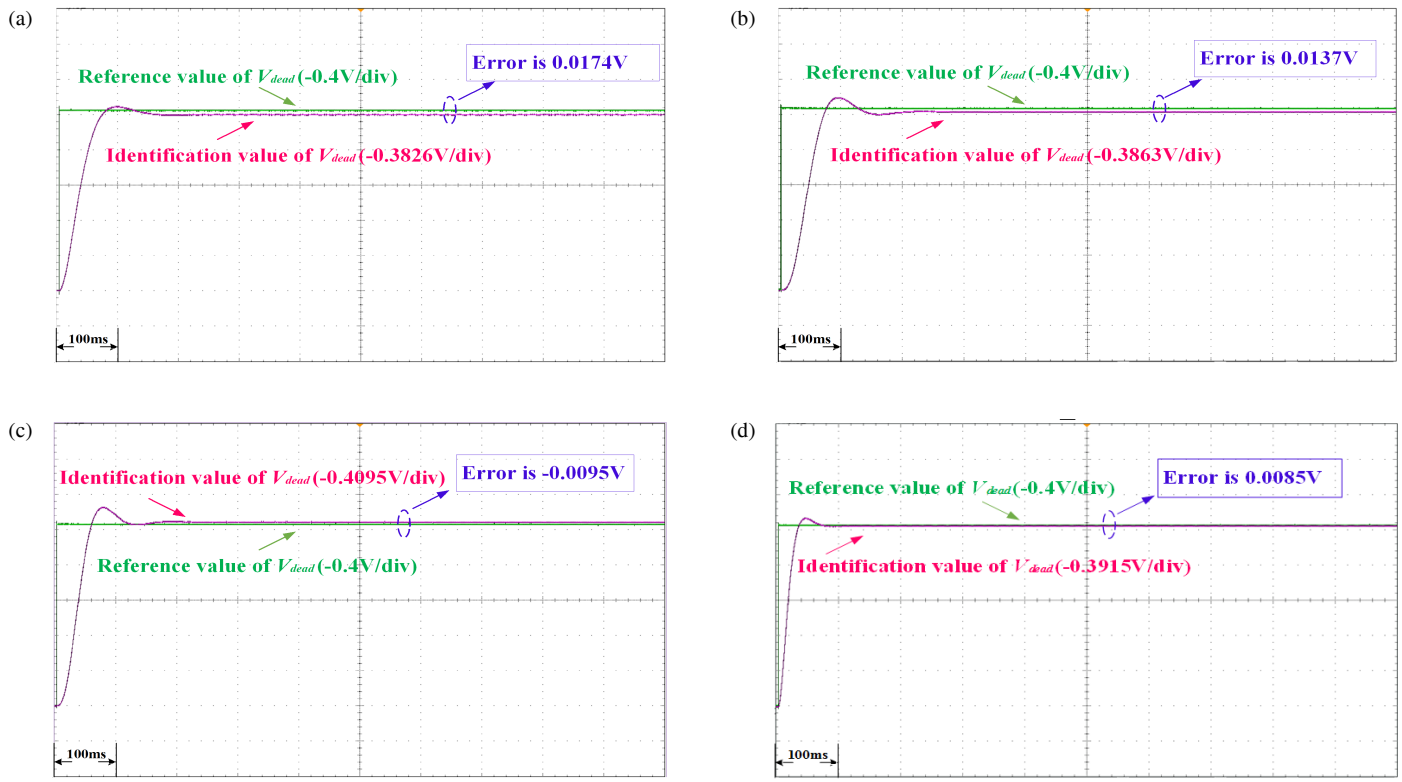

FIGURE 8. The recognition curve of V_{dead}. (a) PSO_$_V$ (100 ms/div) (b) APSO_$_V$ (100 ms/div). (c) AMPSO_$_V$ (100 ms/div). (d) AMBPSO_$_V$ (100 ms/div).

tional real-time performance by regulating the dynamic balance between exploitation and exploration.

Similar to the identification method for R_s, L_s, and ψ_f, the identification result for V_{dead} is presented in Fig. 8. The recognized values under the three improved methods (APSO_$_V$, AMPSO_$_V$, AMBPSO_$_V$) are -0.3863, -0.4095, and -0.3915, respectively. After introducing the adaptive inertia weight and Cauchy mutation mean optimal position improvement strategy, the algorithm's waveform amplitude was increased, and the completion time was shortened. The strategy in which the particles are adjusted according to the size of the fitness and the mean position after mutation is conducive to increasing search ability and improving search efficiency. In addition, the model is considered robust, as a result of the introduction of the environment-seeking capability, which is a consequence of the hybrid BAS.

The analysis of the experimental data using the five identification methods is presented in Table 3.

The comprehensive experimental effect diagram and the data analysis in the above table show that the PMSM parameter identification under the elementary particle swarm method has the problems of large identification error, long identification time, and low robustness. After considering the distortion voltage of the VSI, both the discrimination accuracy and the time required are improved compared to the elementary particle swarm algorithm. On this basis, the improved APSO_$_V$ improves the traditional fixed and unchanging inertia weights into adaptive inertia weights that vary with the average adaptive size, which improves the contraction speed of the particles and narrows the error accuracy to 3–4%. The AMPSO_$_V$ strategy takes into account the optimization results of all particles, thereby reducing the probability of the algorithm falling into a suboptimal solution. AMBPSO_$_V$ introduces the beetle antenna search mechanism compared with AMPSO_$_V$, and the convergence time of the particles is shortened because of its ability to judge the environment. The accuracy and robustness of the three different improvement strategies (APSO_$_V$, AMPSO_$_V$, AMBPSO_$_V$) are improved in comparison to the conventional PSO and PSO_$_V$ recognitions. Moreover, sequentially improving the previous one, the final algorithm obtained (AMBPSO_$_V$) is optimal in terms of discrimination accuracy, convergence time, robustness, etc. The identification error of the flux under AMBPSO_$_V$ is the lowest, 1.7333%; the identification error of the inductor is 2.5860%; and the overall error range is reduced to about 2%.

(2) Disturbance experiment

To further verify the anti-interference capability of the AMBPSO_$_V$ algorithm, experimental validation was conducted under noise disturbance conditions. The experimental results are shown in Fig. 9 and Table 4.

By comparing the identification results under noise-free and noisy conditions, it can be observed that after noise is introduced, the error percentages of the resistance, inductance, flux linkage, and distorted voltage are 2.15%, 2.30%, 2.10%, and 2.25%, respectively. Compared with the corresponding values of 1.9535%, 2.2134%, 1.7333%, and 2.1250% under noise-free

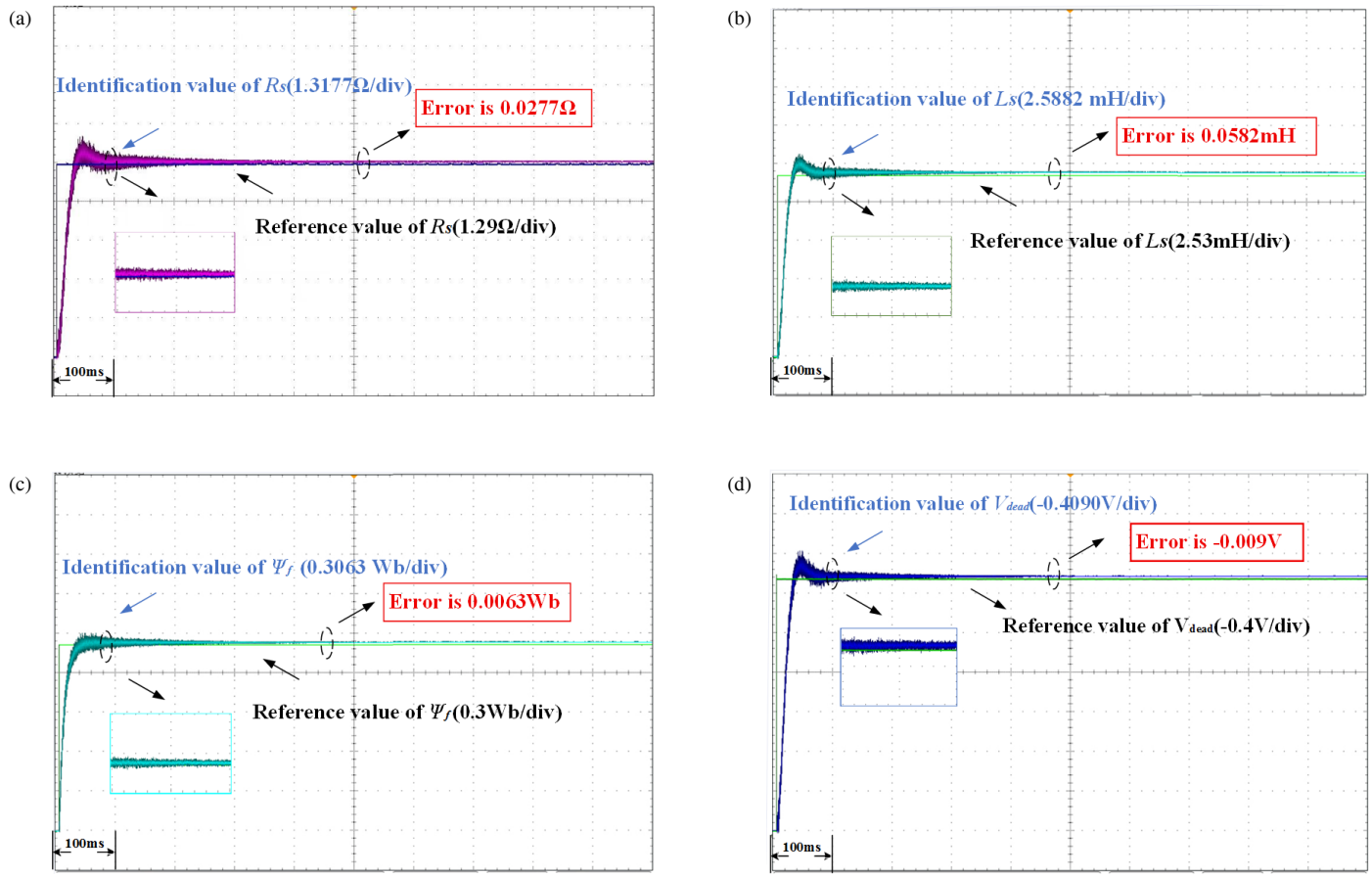

FIGURE 9. Parameter identification results under noise interference conditions. (a) Resistance. (b) Inductance. (c) Flux linkage. (d) Distortion voltage.

TABLE 4. Motor parameter identification values and error rates under disturbance experimental conditions.

Parameter	R_s (Ω)	L_s (mH)	ψ_f (Wb)	V_{dead} (V)
Identification value	1.3177	2.5882	0.3063	−0.4090
Error value	0.0277	0.0582	0.063	−0.0090
Error percentage	2.15%	2.30%	2.10%	2.25%

conditions, the errors only increase slightly, indicating that the noise does not cause a significant deviation in the identification results. This demonstrates that when the measured signals are subjected to random disturbances, the AMBPSO_V algorithm can effectively suppress the influence of noise on the parameter optimization process and avoid particles falling into local misjudgment regions caused by noise, thereby maintaining stable global search capability and convergence accuracy.

The main reason for this result is that, based on the consideration of VSI nonlinear distorted voltage, the AMBPSO_V algorithm further integrates adaptive weight adjustment, average-position guidance, and the beetle antennae search perturbation mechanism. On the one hand, the compensation of VSI distorted voltage reduces the influence of voltage model mismatch on parameter identification. On the other hand, the adaptive search strategy can dynamically adjust the balance between global exploration and local exploitation according to the iterative state, thereby enhancing the algorithm stability in noisy environments. Meanwhile, the beetle antennae search mechanism improves the ability of particles to escape from local optima, enabling the algorithm to effectively search around the true parameter region even under noise interference.

In summary, the AMBPSO_V algorithm can still maintain the identification errors of all parameters within a low range under noise interference, and the error variation is relatively small compared with that under noise-free conditions. This indicates that the proposed algorithm possesses good anti-noise interference capability and parameter identification robustness, and can meet the accuracy requirements of PMSM multi-parameter identification under complex operating conditions.

7. CONCLUSION

In this study, a parameter identification method based on AMBPSO for permanent magnet synchronous motors considering VSI nonlinearities is proposed. The method can identify motor parameters and distortion voltage in real time and has significant advantages in terms of robustness and fast convergence. The following conclusions were drawn from the simulation and experimental comparative analyses.

1) Taking the VSI distortion voltage into account can reduce the voltage model mismatch caused by inverter nonlinearity. Without distortion voltage compensation, the voltage error induced by the inverter may be incorrectly absorbed into the estimated motor parameters, resulting in increased deviations in motor parameter identification. By simultaneously identifying the distortion voltage and motor parameters, the proposed model improves the consistency between the actual PMSM drive system and the identification model, thereby enhancing the parameter identification accuracy.

2) The adaptive inertia weight strategy improves the balance between global exploration and local exploitation. Particles with poorer fitness retain stronger global search capability, while particles close to the optimal region focus more on local refinement. This dynamic adjustment accelerates convergence and improves the stability of the identification process compared with the fixed-weight PSO method.

3) The improved Cauchy mutation mean optimal position strategy enhances the global search ability and reduces the probability of the population falling into suboptimal solutions. This strategy satisfies the diversity and search range of the population.

4) After incorporating the BAS algorithm, the particles are able to perceive the search environment. The particle adjusts the step size according to the environmental judgment during the search process, which significantly improves identification accuracy.

5) Simulated and RT-LAB experimental results verify that the proposed AMBPSO_V method achieves better identification accuracy and faster convergence than the basic PSO and other improved PSO methods. The maximum identification error is reduced by 5.7%, and the convergence time is shortened by 129 ms, demonstrating the feasibility of the proposed method for engineering applications.

ACKNOWLEDGEMENT

This work was supported by the Scientific Research Fund of Hunan Provincial Education Department under Grant Number 24A0395.

REFERENCES

[1] Levi, E., "Advances in converter control and innovative exploitation of additional degrees of freedom for multiphase machines," *IEEE Transactions on Industrial Electronics*, Vol. 63, No. 1, 433–448, Jan. 2016.

[2] Dutta, R. and M. F. Rahman, "Design and analysis of an interior permanent magnet (IPM) machine with very wide constant power operation range," *IEEE Transactions on Energy Conversion*, Vol. 23, No. 1, 25–33, Mar. 2008.

[3] Paramonov, A., S. Oshurbekov, V. Kazakbaev, V. Prakht, V. Dmitrievskii, and V. Goman, "Comparison of differential evolution and Nelder-Mead algorithms for identification of line-start permanent magnet synchronous motor parameters," *Applied Sciences*, Vol. 13, No. 13, 7586, Jun. 2023.

[4] Sun, X., Z. Huang, Z. Yang, G. Lei, and T. Li, "Improved model-free predictive current control for suppressing inverter nonlinearity and parametric time-varying of PMSM drive systems," *IEEE Transactions on Industrial Electronics*, Vol. 72, No. 10, 9866–9875, Oct. 2025.

[5] Zhang, L., J. Ma, Q. Wu, Z. He, T. Qin, and C. Chen, "Research on pmsm speed performance based on fractional order adaptive fuzzy backstepping control," *Energies*, Vol. 16, No. 19, 6922, Oct. 2023.

[6] Liu, K., Q. Zhang, J. Chen, Z. Q. Zhu, and J. Zhang, "Online multiparameter estimation of nonsalient-pole PM synchronous machines with temperature variation tracking," *IEEE Transactions on Industrial Electronics*, Vol. 58, No. 5, 1776–1788, May 2011.

[7] Jin, N.-Z., H.-C. Chen, D.-Y. Sun, Z.-Q. Wu, K. Zhou, and L. Zhang, "Virtual signal injection maximum torque per ampere control based on inductor identification," *Energies*, Vol. 15, No. 13, 4851, Jul. 2022.

[8] Kang, D.-H., H.-K. Kim, J.-K. Park, S.-H. Hyun, and J. Hur, "Demagnetization detection for IPM-type BLDCMs according to irreversible demagnetization patterns and pole-slot coefficients," *Journal of Power Electronics*, Vol. 16, No. 1, 48–56, 2016.

[9] Yoon, J.-S., K.-G. Lee, J.-S. Lee, and K.-B. Lee, "Off-line parameter identification of permanent magnet synchronous motor using a goertzel algorithm," *Journal of Electrical Engineering & Technology*, Vol. 10, No. 6, 2262–2270, 2015.

[10] Rahimi, A., F. Bavafa, S. Aghababaei, M. H. Khooban, and S. V. Naghavi, "The online parameter identification of chaotic behaviour in permanent magnet synchronous motor by self-adaptive learning bat-inspired algorithm," *International Journal of Electrical Power & Energy Systems*, Vol. 78, No. 3, 285–291, 2016.

[11] Cheng, Z., C. Zhang, and Y. Zhang, "Identification of VNS-AGA permanent magnet synchronous wind generator parameters considering magnetic saturation and VSI compensation," *Progress In Electromagnetics Research C*, Vol. 134, 181–195, 2023.

[12] Zhou, Y., S. Zhang, C. Zhang, X. Li, X. Li, and X. Yuan, "Current prediction error based parameter identification method for spmsm with deadbeat predictive current control," *IEEE Transactions on Energy Conversion*, Vol. 36, No. 3, 1700–1710, Sep. 2021.

[13] Li, X. and R. Kennel, "General formulation of Kalman-filter-based online parameter identification methods for VSI-fed PMSM," *IEEE Transactions on Industrial Electronics*, Vol. 68, No. 4, 2856–2864, Apr. 2021.

[14] Yu, Y., X. Huang, Z. Li, M. Wu, T. Shi, Y. Cao, G. Yang, and F. Niu, "Full parameter estimation for permanent magnet synchronous motors," *IEEE Transactions on Industrial Electronics*, Vol. 69, No. 5, 4376–4386, May 2022.

[15] Huang, Y., J. Zhang, D. Chen, and J. Qi, "Model reference adaptive control of marine permanent magnet propulsion motor based on parameter identification," *Electronics*, Vol. 11, No. 7, 1012, 2022.

[16] Prabhakaran, K. K. and A. Karthikeyan, "Electromagnetic torque-based model reference adaptive system speed estimator

for sensorless surface mount permanent magnet synchronous motor drive," *IEEE Transactions on Industrial Electronics*, Vol. 67, No. 7, 5936–5947, Jul. 2020.

[17] Cheng, Z., C. Zhang, and Y. Zhang, "PMSWG parameter identification method based on improved operator genetic algorithm," *Progress In Electromagnetics Research C*, Vol. 139, 67–77, 2024.

[18] Zhu, Y., Q. Chen, K. Li, W. Yang, and Y. Huang, "Parameter identification of interior permanent magnet synchronous based on local search-based hybrid genetic algorithm," *Journal of Electromagnetic Waves and Applications*, Vol. 36, No. 9, 1311–1322, 2022.

[19] Peesapati, R., Anamika, and N. Kumar, "Electricity price forecasting and classification through wavelet–dynamic weighted PSO–FFNN approach," *IEEE Systems Journal*, Vol. 12, No. 4, 3075–3084, Dec. 2018.

[20] Zhou, S., D. Wang, and Y. Li, "Parameter identification of permanent magnet synchronous motor based on modified-fuzzy particle swarm optimization," *Energy Reports*, Vol. 9, 873–879, Mar. 2023.

[21] Liu, Z.-H., H.-L. Wei, X.-H. Li, K. Liu, and Q.-C. Zhong, "Global identification of electrical and mechanical parameters in PMSM drive based on dynamic self-learning PSO," *IEEE Transactions on Power Electronics*, Vol. 33, No. 12, 10 858–10 871, Dec. 2018.

[22] Zhang, Y., M. Zhou, C. Zhang, A. Shen, and L. Bing, "Identification of PMSM parameters with time-error compensated based on contractile factor antipredator PSO," *IEEE Transactions on Transportation Electrification*, Vol. 10, No. 2, 4006–4017, Jun. 2024.

[23] Jiang, X. and S. Li, "BAS: Beetle antennae search algorithm for optimization problems," *International Journal of Robotics and Control*, Vol. 1, No. 1, 2018.

[24] Zhang, B., P. Niu, X. Guo, and J. He, "Fuzzy PID control of permanent magnet synchronous motor electric steering engine by improved beetle antennae search algorithm," *Scientific Reports*, Vol. 14, No. 1, 2898, Feb. 2024.

[25] Yu, X.-w., L.-p. Huang, Y. Liu, K. Zhang, P. Li, and Y. Li, "WSN node location based on beetle antennae search to improve the gray wolf algorithm," *Wireless Networks*, Vol. 28, No. 2, 539–549, 2022.

[26] Feng, T., S. Deng, Q. Duan, and Y. Mao, "Application of local search particle swarm optimization based on the beetle antennae search algorithm in parameter optimization," in *Actuators*, Vol. 13, No. 7, 270, Jul. 2024.